Space-time-resolved quantum field approach to Klein-tunneling dynamics across a finite barrier

M. Alkhateeb and A. Matzkin ⬤

Laboratoire de Physique Théorique et Modélisation, CNRS Unité 8089, CY Cergy Paris Université, 95302 Cergy-Pontoise Cedex, France

We investigate Klein tunneling through finite potential barriers with space-time-resolved solutions to relativistic quantum field equations. We find that no particle actually tunnels through a finite supercritical barrier, even in the case of resonant tunneling. The transmission is instead mediated by modulations in pair production rates, at each edge of the barrier, caused by the incoming electron. We further examine the effect of the barrier's width on the numbers of produced pairs in the fermionic case (characterized by saturation) and in the bosonic case (characterized by exponential superradiance). This work paves the way to precise studies of the radiating dynamics of supercritical barriers, and could be applied to certain analogs of Klein tunneling observed in systems modeled by relativistic wave equations.

Vacuum pair production in a strong supercritical external field is one of the basic elementary processes predicted by relativistic quantum theory [1,2]. Understanding its precise dynamics is important not only for fundamental reasons, but also due to current efforts aiming to experimentally observe pair production in the intense laser facilities currently under construction [3,4]. To this end, several works employing different approaches have examined field configurations that would optimize pair production [5–8].

A related aspect concerns the interaction of a charged particle with the pair production process as the particle scatters on an inhomogeneous supercritical field. This is well known to give rise to "Klein tunneling" [9], that in a first quantized framework appears as undamped propagation inside the potential region. The precise dynamics of this interaction has remained controversial even in the case of a simple electrostatic step, a situation giving rise to the so-called Klein paradox [10]. Time-independent first quantized approaches are generally misleading [11], but even stationary quantum field theory (QFT) methods failed to reach a consensus (e.g., the choice of asymptotic "in" and "out" fields [12–15]). A numerical space-time-resolved QFT approach [16] was instrumental in computing the precise dynamics of the interaction between the incoming particle and the pair production for a step, leading to a reinterpretation of the fermionic Klein paradox in terms of the Pauli blockade of vacuum pair production.

For a particle impinging on a supercritical electrostatic barrier of finite width, the computation of the time-dependent pair creation rates and of the dynamics inside the barrier is expected to be more involved; in particular the asymptotic field operators only contain particles, which has led some authors [9,17] to conjecture that a symmetric supercritical barrier once formed cannot radiate. While genuine Klein tunneling has yet to be observed for elementary particles, the physics encapsulated in the first quantized Dirac equation has been used as an effective model in other areas, leading to the experimental observation of Klein tunneling in graphene heterojunctions

[18], with photonic crystals [19], trapped ions [20], or cold quantum gases [21].

In this Letter, we implement a time-dependent space-resolved QFT treatment in order to compute the detailed dynamics of Klein tunneling for fermions and bosons across a finite barrier. In the fermionic case, the calculations will lead us to propose a mechanism accounting for the undamped transmission characterizing Klein tunneling: Due to the exchange symmetry, pair production appears only as a transient effect when the field is turned on. A particle incoming on the saturated barrier then induces modulations in the antiparticle density which in turn triggers production of the transmitted particle. Hence no particle actually tunnels inside the barrier, even in the resonant case of nearly full transmission. In the bosonic case, a barrier amplifies pair production, with the antiboson charge oscillating inside the barrier increasing exponentially each time it scatters on an edge.

The barrier is modeled as a one-dimensional background external field with negligible backreaction [22]. The fermionic pair production rate is obtained from field operators Ψ expanded as

$$\Psi(x,t) = \int dp[b_p(t)\phi_p(x) + d_p^\dagger(t)\varphi_p(x)]. \tag{1}$$

ϕ_p and φ_p are respectively the positive and negative energy spinor eigenfunctions of the field-free Dirac Hamiltonian $H_0 = -i\hbar c\alpha_x\partial_x + \beta mc^2$ with eigenvalues $\pm|E_p| = \pm\sqrt{p^2c^2 + m^2c^4}$ (α and β are the usual Dirac matrices [23], m the electron mass, and c the light velocity), $b_p(t)$ [respectively $d_p(t)$] is the annihilation operator for a particle (respectively antiparticle), and $b_p^\dagger(t)$ and $d_p^\dagger(t)$ are the corresponding creation operators obeying the usual commutation relations, i.e., the only nonzero equal time anticommutators are $[b_p, b_k^\dagger]_+ = [d_p, d_k^\dagger]_+ = \delta(p-k)$. The time dependence of the creation and annihilation operators is obtained by noting that Ψ obeys the Dirac equation with the full Hamiltonian $H = H_0 + V(x)$,

where $V(x)$ is the background potential. It then follows that [24]

$$b_p(t) = \int dk [U_{\phi_p \phi_k}(t) b_k(0) + U_{\phi_p \varphi_k}(t) d_k^\dagger(0)], \qquad (2)$$

$$d_p^\dagger(t) = \int dk [U_{\varphi_p \phi_k}(t) b_k(0) + U_{\varphi_p \varphi_k}(t) d_k^\dagger(0)]. \qquad (3)$$

The time-evolved amplitudes, defined by

$$U_{\phi_k \varphi_p}(t) \equiv \langle \phi_k | \exp(-iHt/\hbar) | \varphi_p \rangle, \qquad (4)$$

are computed numerically on a discretized space-time grid by relying on a split operator [25] method: The evolution operator is split into a kinetic part propagated in momentum space and a potential-dependent part solved in position space [26].

Let us first consider vacuum pair production in a quasirectangular potential barrier of width L; for definiteness we take $V(x) = \frac{V_0}{2} \{\tanh[(x + L/2)/\epsilon] - \tanh[(x - L/2)/\epsilon]\}$, where $V_0 > 2mc^2$ is supercritical and ϵ is a smoothness parameter. The electron density is obtained from the vacuum expectation value $\rho_{\mathrm{el}}(x, t) = \langle 0 | \Psi_{\mathrm{el}}^\dagger(x, t) \Psi_{\mathrm{el}}(x, t) | 0 \rangle$, where Ψ_{el} is the positive energy part of Eq. (1). The positron density $\rho_{\mathrm{pos}}(x_1, x_2, t)$ is obtained similarly from Ψ_{pos} defined as the positive energy part of the field conjugate to the one given by Eq. (1) [27]. It should be stressed that such densities (in particular the positron densities) represent particle densities in a field-free basis [28]. This corresponds to an experiment in which the particles would be counted after switching off the field instantaneously.

Since a potential of the form $V(x)$ typically creates two pairs simultaneously (one at edge of the barrier, where the field is highly inhomogeneous), it is particularly instructive to compute the two-particle density for a joint electron or positron creation at x_1 and x_2,

$$\rho_{\mathrm{a}}(x_1, x_2, t) = \langle 0 | \Psi_{\mathrm{a}}^\dagger(x_1, t) \Psi_{\mathrm{a}}^\dagger(x_2, t) \Psi_{\mathrm{a}}(x_2, t) \Psi_{\mathrm{a}}(x_1, t) | 0 \rangle / 2!, \qquad (5)$$

where "a" stands for pos or el. Note that by construction $\rho(x_1, x_2)$ also counts the number of multiple pairs created on the same edge of the barrier, although the probability for multiple pair creations at a single field inhomogeneity is expected to decrease exponentially as the multiplicity number increases [29,30] (but see Ref. [31]). The two-particle density (5) can be shown to be written as [26]

$$\rho_{\mathrm{a}}(x_1, x_2, t) = \rho_{\mathrm{a}}(x_1, t) \rho_{\mathrm{a}}(x_2, t)/2 - \rho_{\mathrm{a}}^{\mathrm{int}}(x_1, x_2, t), \qquad (6)$$

indicating that the number of created pairs is affected by the exchange interaction terms encapsulated in ρ^{int}. This is portrayed in Fig. 1 for the positron density inside the barrier. As the positrons produced at each edge propagate towards the opposite side, $\rho_{\mathrm{pos}}^{\mathrm{int}}$ becomes of the same order of magnitude as the factorized density $\rho_{\mathrm{pos}}(x_1) \rho_{\mathrm{pos}}(x_2)$, so that the exchange interaction significantly reduces the number of couples inside the barrier.

The number $N(t)$ of created positron-electron pairs, obtained by integrating either $\rho_{\mathrm{pos}}(x, t)$ or $\rho_{\mathrm{el}}(x, t)$ over all space (i.e., essentially inside the barrier for ρ_{pos}, outside for ρ_{el}) is shown in Fig. 2(a) for different barrier widths. $N(t)$ is seen to saturate after a transient time that depends on the barrier width: At short times the number of produced pairs increases
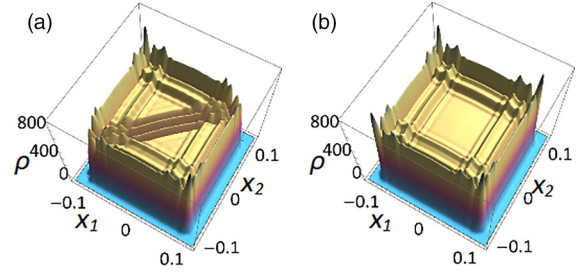

FIG. 1. (a) The spatial density $\rho(x_1, x_2)$ of positron couples at positions x_1 and x_2 created inside the barrier at time 2×10^{-3} expressed in atomic units (a.u., defined by $\hbar = m = 1$, $c = 137.036$, where m is the electron mass); the barrier has width $L = 0.2$ a.u., height $V_0 = 3mc^2$, and the smoothness has been set to $\epsilon = 0.3/c$. (b) Same as (a) but without the exchange interaction terms in the computations [see Eq. (6)].

similarly to a step potential, but a fermionic symmetric barrier will not radiate after this transient period, as expected from the asymptotic behavior of the evolution amplitudes $U_{\phi_k \varphi_p}(t)$ [32].

We can now examine how an electron colliding on the supercritical barrier interacts with the fermionic pair production process. We will consider resonant Klein tunneling, that has been widely investigated in the condensed matter analog of quasiparticles undergoing nearly full transmission through electrostatic barriers in graphene [33]. The field operators are again given by Eqs. (1)–(3), but the spatial densities are obtained from the expectation values

$$\rho_{\mathrm{a}}(x) = \langle \zeta | \Psi_{\mathrm{a}}^\dagger(x) \Psi_{\mathrm{a}}(x) | \zeta \rangle, \qquad (7)$$

where $|\zeta\rangle = \int dp \zeta_p(p_0, x_0) b_p^\dagger(0) |0\rangle$ represents the initial electron wave packet centered at x_0 with mean momentum p_0; for definiteness we take $\zeta_p(p_0, x_0) \propto e^{-\Delta^2(p-p_0)^2 - ipx_0/\hbar}$ corresponding to a Gaussian wave packet of width Δ, similarly to previous works dealing with the Klein paradox due to a
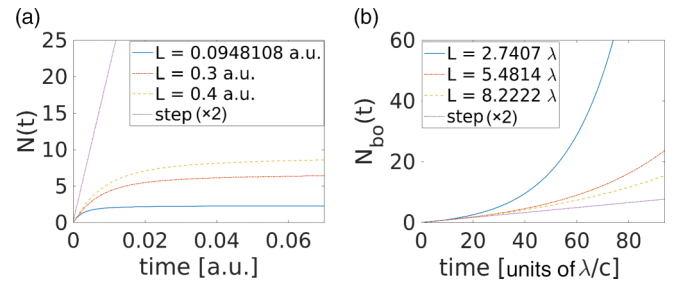

FIG. 2. (a) Time dependence (in a.u.) of the total number of created electron-positron pairs $N(t)$ for a fermionic barrier with the parameters given in Fig. 1 except for the width L, indicated in the legend. The rate vanishes except in the limit of a potential step (note that in order to compare the step and finite barrier cases, the curve shown for a step has been multiplied by two). (b) The total number of created boson-antiboson pairs $N_{\mathrm{bo}}(t)$ for a massive bosonic field obeying the Klein-Gordon equation interacting with a background potential barrier with $V_0 = 3m_{\mathrm{bo}}c^2$, $\epsilon = 0.3/c$, and varying widths; m_{bo} is the boson mass which renormalizes the atomic units, so that L and t are given in units of $\lambda = m_{\mathrm{bo}}\hbar/c$ and λ/c, respectively.

potential step [16,34]. The resonant barrier condition [35]

$$\left(p_0^2 + V^2/c^2 - 2V\sqrt{p_0^2/c^2 + m^2}\right)^{1/2} = \frac{k\pi}{2L} \quad (8)$$

(which holds for a rectangular barrier, corresponding to the potential slope parameter $\epsilon \to 0$) is obtained by maximizing the transmitted Dirac current relative to the incident one (k is an integer). In the first quantized approach, this means that the transmission amplitude $T(p_0)$ for stationary solutions of the Dirac equation is unity, so that if the wave packet is sufficiently narrow in momentum, it will nearly entirely tunnel through the barrier [11].

However, in the present more fundamental second quantized framework, the incoming electron interplays with the particles created by the supercritical potential. The electronic spatial density given by Eq. (7) can be shown [26] to take the form, by using Eqs. (1)–(3), $\rho_{\text{el}} = \langle 0|\Psi_{\text{el}}^\dagger \Psi_{\text{el}}|0\rangle + \rho_{\text{el}}^\zeta$, where

$$\rho_{\text{el}}^\zeta(x) = \left|\int dp\,dk\,\zeta(p)U_{\phi_k\phi_p}(t)\phi_k(x)\right|^2 \quad (9)$$

gives the evolution of the wave-packet density. Inside the barrier the electron density vanishes (hence there is no electron wave packet) and the positron density reads

$$\rho_{\text{pos}}(x,t) = \langle 0|\Psi_{\text{pos}}^\dagger(x,t)\Psi_{\text{pos}}(x,t)|0\rangle - \rho_{\text{pos}}^\zeta(x,t), \quad (10)$$

where the last term

$$\rho_{\text{pos}}^\zeta(x) = \left|\int dp\,dk\,\zeta(p)U_{\varphi_k\phi_p}(t)\varphi_k(x)\right|^2 \quad (11)$$

appears as a correction to the vacuum positron density due to the incoming electron scattering on the supercritical potential [26].

In the case of resonant Klein tunneling, the barrier needs to be narrow relative to the wave-packet width, so this decrease will be small, but it is nevertheless crucial in order to modulate pair production at the right edge of the barrier. Indeed, most of the wave packet will typically reach the barrier at times for which the pair production rate becomes negligible. The mechanism invoked in Ref. [16] explaining the Klein paradox for a supercritical step as the result of Pauli blockade should be parsed differently for a finite barrier since a sizable part of the wave packet will typically reach the barrier at times for which the pair production rate vanishes. A mechanism consistent with our computations could be the following: (i) The incoming electron annihilates a barrier positron [36], depleting the positron density, thereby creating a dip. (ii) The dip propagates inside the barrier; physically, the positrons' motion is opposite to that of the dip, as the states of the annihilated positrons become unoccupied. (iii) Upon reaching the right edge, the dip stimulates pair production. (iv) The created electrons at the right edge of the barrier account for the recreated transmitted wave packet. Note that the depletion instability undergoes multiple reflections inside the barrier, with successively decreasing amplitudes [11]. Hence when the positron density dip reaches the left edge, pair production is stimulated and the resulting created electronic charge contributes to the small reflected wave packet.

Numerical results illustrating resonant Klein tunneling are given in Fig. 3. Each panel shows snapshots at different
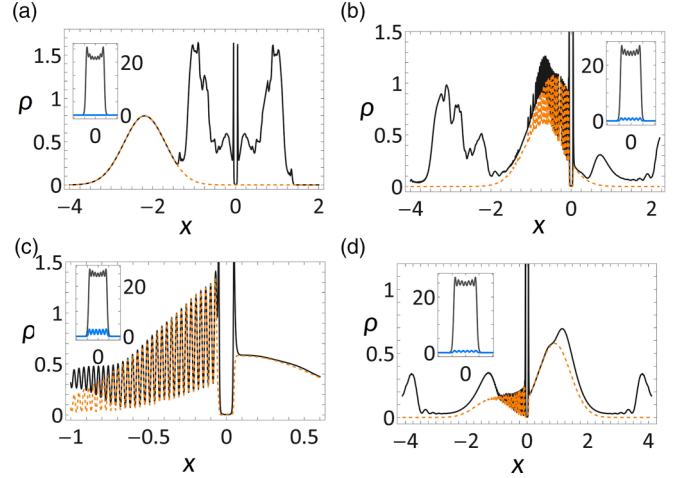

FIG. 3. Dynamics of Klein tunneling: An electron wave packet initially ($t = 0$) centered at $x = -3$ a.u. to the left of the supercritical barrier is launched with mean momentum $p_0 = 100$ a.u. The barrier ($V_0 = 3mc^2$, $\epsilon = 0.3/c$) lies in the region $-0.0474 < x < 0.0474$ a.u., chosen so that the width L obeys the resonance condition [Eq. (8)]. (a) Snapshot of particle densities at $t = 10^{-2}$ a.u., as the electron wave packet (dotted orange line) approaches the barrier. The solid black line gives the total electron density (due to pair creation as well as the wave packet). The positron density lies outside the scale of the main plot and is shown in the inset (thick gray line); the thin blue line is the contribution of the modulations due to the interaction between the wave packet and the barrier. (b) Snapshot at $t = 3\times10^{-2}$ a.u. as the wave packet reaches the barrier. (c) Zoom around the barrier region at $t = 4\times10^{-2}$ a.u., as the electron wave packet is reformed at the right edge of the barrier; note there is no electron density inside the barrier, but the positron modulations (thin line in the inset) are of greater amplitude. (d) At $t = 5\times10^{-2}$ a.u. most of the wave packet (dotted orange line) is "transmitted" to the right, while a smaller fraction is reflected.

times. By the time the initial electron wave packet [Fig. 3(a)] reaches the barrier, the pair production rate has already decreased [Fig. 3(b)]. A small part of the electron wave packet is reflected, while the transmitted part annihilates barrier positrons, thereby modulating the positron density inside the barrier [Fig. 3(c)]. Note there is no electron inside the barrier (the electron density is vanishingly small). The electron wave packet is then reformed at the right edge of the barrier [Fig. 3(d)] by pair creation due to the positron modulation. Hence there is no tunneling in Klein tunneling, but a change in the pair creation rate at both edges of the barrier caused by the incoming electron. Another example detailing the barrier dynamics for a wider and parsing each step of the proposed mechanism is shown in Fig. 4.

The present QFT formalism can be applied similarly to spin-0 bosons obeying the Klein-Gordon equation. The field operators in Eqs. (1)–(3) now obey commutation rules, and the basis functions ϕ_p and φ_p are two-component solutions of the free Klein-Gordon equation expressed in Hamiltonian form [10]. As is well known, bosons scattering on a supercritical potential step give rise to superradiance [37], whereby the bosonic amplitude reflected from the step is larger than the incoming one [38] (compensated inside the step by the creation of antibosonic amplitude). The same phenomenon in
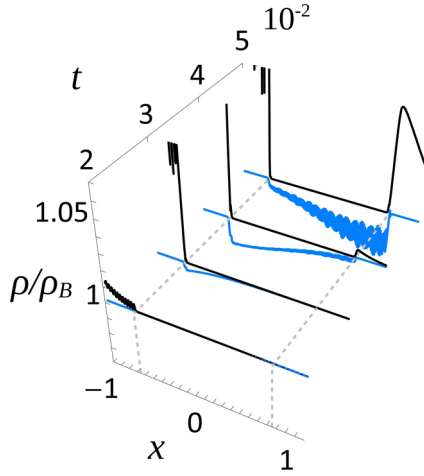
FIG. 4. The transmission mechanism detailed in the text is illustrated for an electron wave packet colliding on a smooth rectangular barrier (region between dashed lines, x in a.u.). The ratio $\rho_{el}(x, t)/\rho_{B\,el}(x, t)$ is shown in black at different times (ρ_{el} is the total electron density and $\rho_{B\,el}$ the electron density in the absence of an incoming wave packet). The corresponding positron number density ratio $\rho_{pos}(x, t)/\rho_{B\,pos}(x, t)$ is shown in gray (online blue). At $t = 2 \times 10^{-2}$ a.u., the front tail of the electron wave packet reaches the left edge of the filled barrier. This creates a dip in the positron density, visible at $t = 3 \times 10^{-2}$ a.u. The dip propagates inside the barrier ($t = 4 \times 10^{-2}$ a.u.), and reaches the right edge, stimulating pair production. The additional created electron excitations (relative to vacuum polarization) to the right of the barrier are seen at $t = 5 \times 10^{-2}$ a.u. to correspond to the front tail of the wave packet that appears as having been transmitted.

the case of a supercritical barrier is expected to lead to an exponential rate of pair creation, as the antibosons created at one edge of the barrier undergo multiple scatterings inside the barrier. Our numerical results, shown in Fig. 2(b) for increasing barrier widths, confirm this behavior. For a fixed potential, the momentum distribution of the ejected bosons peaks at $(V_0^2 - 4m^2c^4)^{1/2}/2c$, so the creation rate only depends on the

time taken by the antibosons to travel from one edge to the other. A similar self-amplification takes place in supercritical wells [39] and can be traced back to the divergent behavior of the scattering amplitudes when interacting with a field inhomogeneity [40].

Note that in the case of bosonic Klein tunneling, the incoming boson will also undergo an amplification by multiple scattering inside the barrier; the total antiboson (ab) density inside the barrier takes the form

$$\rho_{ab}(x, t) = \langle 0|\Psi_{ab}^{\dagger}(x, t)\Psi_{ab}(x, t)|0\rangle + \rho_{ab}^{\zeta}(x, t), \quad (12)$$

similar to Eq. (10) but with the sign of the modulation inverted relative to the fermionic case. The incoming boson now enhances pair production when colliding at the left edge of the barrier. The modulation caused by the wave packet, described by the term ρ_{ab}^{ζ} in Eq. (12), propagates inside the barrier, amplifying the charge with each collision on a barrier edge on top of the antibosonic charge produced by the field.

To sum up, we have investigated Klein tunneling across a supercritical barrier employing a space-time-resolved QFT approach. While this approach does not aim at quantitative predictions for a specific future experiment, the present nonperturbative theoretical framework provides an understanding of the elementary processes underlying not only Klein tunneling, but also the radiating properties of the barrier. Concerning the latter, we recovered the expected asymptotic behavior for pair production by a symmetric background potential [9], but have also further unraveled the detailed time-dependent dynamics and correlations for shorter times. Our proposed mechanism describing the undamped tunneling feature when a particle impinges on a finite barrier goes beyond the results obtained previously [16,24] concerning the resolution of the Klein paradox for a potential step, in that the mechanism accounts for particle transmission. Additional refinements, such as the inclusion of the Coulomb repulsion, will be necessary in order to achieve a definitive understanding of tunneling in supercriticial potentials.

[1] R. Ruffini, G. Vereshchagin, and S.-S. Xue, Phys. Rep. **487**, 1 (2010).

[2] A. Fedotov, A. Ilderton, F. Karbstein, B. King, D. Seipt, H. Taya, and G. Torgrimsson, arXiv:2203.00019.

[3] G. V. Dunne, Eur. Phys. J. D **55**, 327 (2009).

[4] H. Hu, Contemp. Phys. **61**, 12 (2020).

[5] I. A. Aleksandrov, G. Plunien, and V. M. Shabaev, Phys. Rev. D **94**, 065024 (2016).

[6] H. Gies and G. Torgrimsson, Phys. Rev. Lett. **116**, 090406 (2016).

[7] J. Unger, S. Dong, Q. Su, and R. Grobe, Phys. Rev. A **100**, 012518 (2019).

[8] D. D. Su, Y. T. Li, Q. Z. Lv, and J. Zhang, Phys. Rev. D **101**, 054501 (2020).

[9] N. Dombey and A. Calogeracos, Phys. Rep. **315**, 41 (1999).

[10] W. Greiner, B. Müller, and J. Rafelski, *Quantum Electrodynamics of Strong Fields* (Springer, Berlin, 1985), Chaps. 5 and 10.

[11] M. Alkhateeb, X. Gutiérrez de la Cal, M. Pons, D. Sokolovski, and A. Matzkin, Phys. Rev. A **103**, 042203 (2021).

[12] A. I. Nikishov, Phys. At. Nucl. **67**, 1478 (2004).

[13] A. Hansen and F. Ravndal, Phys. Scr. **23**, 1036 (1981).

[14] S. P. Gavrilov and D. M. Gitman, Phys. Rev. D **93**, 045002 (2016).

[15] A. Chervyakov and H. Kleinert, Phys. Part. Nucl. **49**, 374 (2018).

[16] P. Krekora, Q. Su, and R. Grobe, Phys. Rev. Lett. **92**, 040406 (2004).

[17] M. J. Thomson and B. H. J. McKellar, Am. J. Phys. **59**, 340 (1991).

[18] A. Young and P. Kim, Nat. Phys **5**, 222 (2009).

[19] X. Jiang, C. Shi, Z. Li, S. Wang, Y. Wang, S. Yang, S. G. Louie, and X. Zhang, Science **370**, 1447 (2020).

[20] R. Gerritsma *et al.*, Phys. Rev. Lett. **106**, 060503 (2011).

[21] T. Salger, C. Grossert, S. Kling, and M. Weitz, Phys. Rev. Lett. **107**, 240401 (2011).

[22] S. P. Gavrilov and D. M. Gitman, Phys. Rev. Lett. **101**, 130403 (2008).

[23] We will consider the usual one effective spatial dimension approximation, neglecting spin flip and replacing α_x and β by the Pauli matrices σ_1 and σ_3, respectively.

[24] T. Cheng, Q. Su, and R. Grobe, Contemp. Phys. **51**, 315 (2010).

[25] M. Ruf, H. Bauke, and C. H. Keitel, J. Comput. Phys. **228**, 9092 (2009).

[26] See Supplemental Material at http://link.aps.org/supplemental/10.1103/PhysRevA.106.L060202 for details.

[27] S. S. Schweber, *An Introduction to Relativistic Quantum Field Theory* (Dover, New York, 2005).

[28] P. Krekora, Q. Su, and R. Grobe, Phys. Rev. A **73**, 022114 (2006).

[29] K. Hencken, D. Trautmann, and G. Baur, Phys. Rev. A **51**, 998 (1995).

[30] T. Cheng, Q. Su, and R. Grobe, Phys. Rev. A **80**, 013410 (2009).

[31] Q. Z. Lv and H. Bauke, Phys. Rev. D **96**, 056017 (2017).

[32] M. Alkhateeb and A. Matzkin (unpublished).

[33] M. I. Katsnelson, K. S. Novoselov, and A. K. Geim, Nat. Phys. **2**, 620 (2006).

[34] M. Ruf, G. R. Mocken, C. Müller, K. Z. Hatsagortsyan, and C. H. Keitel, Phys. Rev. Lett. **102**, 080402 (2009).

[35] N. Dombey, P. Kennedy, and A. Calogeracos, Phys. Rev. Lett. **85**, 1787 (2000).

[36] Recall that the supercritical barrier is modeled as an external unquantized background field that creates and annihilates particles associated with the fermionic field.

[37] C. A. Manogue, Ann. Phys. **181**, 261 (1988).

[38] R. E. Wagner, M. R. Ware, Q. Su, and R. Grobe, Phys. Rev. A **81**, 024101 (2010).

[39] R. E. Wagner, M. R. Ware, Q. Su, and R. Grobe, Phys. Rev. A **81**, 052104 (2010).

[40] M. Alkhateeb and A. Matzkin, Am. J. Phys. **90**, 297 (2022).

Supplementary Material for
Space-time resolved quantum field approach to Klein tunneling dynamics across a finite barrier

M. Alkhateeb[1] and A. Matzkin[1]

[1]*Laboratoire de Physique Théorique et Modélisation, CNRS Unité 8089, CY Cergy Paris Université, 95302 Cergy-Pontoise cedex, France*

1. PARTICLE DENSITIES

We derive here the expressions for the particle number, density and the number of couples starting from the field equations, Eqs. (1)-(3) of the main text. We first derive the expressions starting from the vacuum, and then consider the case of an incoming particle scattering on the barrier. For definitiness we will deal with fermionic fields.

1.1 Vacuum expectation values

Our starting point is the usual expressions [1] for the particle number, number density or number of couples in terms of the field operator $\Psi(x,t)$. For example the particle (say the electron) density is obtained as the vacuum expectation value

$$
\begin{aligned}
\rho_{el}(x,t) &= \langle 0|\hat{\Psi}_{el}^{\dagger}(x,t)\hat{\Psi}_{el}(x,t)|0\rangle \\
&= \langle 0| \int dp\,\phi_p^{\dagger}(x)\hat{b}_p^{\dagger}(t) \int dk\,\hat{b}_k(t)\phi_k(x)|0\rangle
\end{aligned}
\tag{S-1}
$$

Using the Bogoliubov transformation [2] given by Eqs. (2)-(3) of the paper, the time-dependence of the creation and annihilation operators becomes encapsulated in unitary evolution amplitudes. The number density of electrons can then be written as

$$
\begin{aligned}
\rho_{el}(x,t) = \langle 0| \int dp\,\phi_p^{\dagger}(x) \int dp'\big(U_{\phi_p\phi_{p'}}^{*}(t)\hat{b}_{p'}^{\dagger} + U_{\phi_p\varphi_{p'}}^{*}(t)\hat{d}_{p'}\big) \\
\int dk \int dk'\big(U_{\phi_k\phi_{k'}}(t)\hat{b}_{k'} + U_{\phi_k\varphi_{k'}}^{*}(t)\hat{d}_{k'}^{\dagger}\big)\phi_k(x)|0\rangle
\end{aligned}
\tag{S-2}
$$

where the evolution operator is defined in Eq. (4) of the paper. Notice that the terms with $\hat{b}|0\rangle$ and $\langle 0|\hat{b}^{\dagger}$ are vanishing and the surviving terms give the number density:

$$
\rho_{el}(x,t) = \int dp\,dk\,\langle 0| \int dp'\,\hat{d}_{p'}\,U_{\phi_p\varphi_{p'}}^{*}(t)\phi_p^{\dagger}(x)\phi_k(x) \int dk'\,U_{\phi_k\varphi_{k'}}(t)\hat{d}_{k'}^{\dagger}|0\rangle\rangle
\tag{S-3}
$$

Since $\hat{d}_{k'}\hat{d}_{p'}^{\dagger}|0\rangle = \delta_{p',k'}|0\rangle$ the number density becomes:

$$
\begin{aligned}
\rho_{el}(x,t) &= \int dp\,dk \int dk'\,U_{\phi_p\varphi_{k'}}^{*}(t)\phi_p^{\dagger}(x)\phi_k(x)U_{\phi_k\varphi_{k'}}(t) \\
&= \int dk \left| \int dp\,U_{\phi_p\varphi_k}(t)\phi_p(x) \right|^2 .
\end{aligned}
\tag{S-4}
$$

The number of created electrons at time t can be obtained by integrating Eq. (S-4) with with respect to x:

$$
N_{el}(t) = \int dp\,dk \left| U_{\phi_p\varphi_k}(t) \right|^2
\tag{S-5}
$$

The electron number is shown in Fig. 2(a) of the main text for varying barrier widths.

In the same way, one can obtain the number density of positrons (see Figs. 3 and 4 of the main text). The corresponding expressions are

$$
\rho_{po}(x,t) = \int dpdk \langle 0| \hat{d}_p^\dagger(t) \varphi_p^\dagger(x) \varphi_k(x) \hat{d}_k(t) |0\rangle
$$
$$
= \int dp \left| \int dk U_{\varphi_k \phi_p}(t) \varphi_k(x) \right|^2
$$
(S-6)

and the number of the created positrons:

$$
N_{po} = \int dpdk \left| U_{\varphi_k \phi_p}(t) \right|^2
$$
(S-7)

In the barrier problem, the number density for the particle couples found at positions x_1 and x_2 given by Eq. (5) of the text is an interesting quantity, as we are dealing with two field inhomogeneities. By employing the same techniques and recalling that states denoted $|p_1, p_2\rangle$ are Fock space states, the couple density is given by

$$
\rho_{el}(x_1, x_2, t) = \langle 0| \hat{\Psi}_{1el}^\dagger(x_1,t) \hat{\Psi}_{2el}^\dagger(x_2,t) \hat{\Psi}_{2el}(x_2,t) \hat{\Psi}_{1el}(x_1,t) |0\rangle
$$
$$
= \int dp_1 \ldots dp_4 \langle 0| \phi_{p_1}^\dagger(x_1) \phi_{p_2}^\dagger(x_2) \hat{b}_{p_1}^\dagger(t) \hat{b}_{p_2}^\dagger(t)
$$
$$
\hat{b}_{p_3}(t) \hat{b}_{p_4}(t) \phi_{p_3}(x_2) \phi_{p_4}(x_1) |0\rangle
$$
(S-8)

One can now use the expressions of the time dependence of the creation and annihilation operators, Eq. (2) and by keeping only the surviving terms, one obtains:

$$
\rho_{el}(x_1, x_2, t) = \int dp_1 \ldots dp_4 dk_1 \ldots dk_4 \langle 0| U_{\phi_{p_1}, \varphi_{k_1}}^*(t) U_{\phi_{p_2}, \varphi_{k_2}}^*(t) U_{\phi_{p_3}, \varphi_{k_3}}(t) U_{\phi_{p_4}, \varphi_{k_4}}(t)
$$
$$
\hat{d}_{k_1} \hat{d}_{k_2} \hat{d}_{k_3}^\dagger \hat{d}_{k_4}^\dagger \phi_{p_1}^\dagger(x_1) \phi_{p_2}^\dagger(x_2) \phi_{p_3}(x_2) \phi_{p_4}(x_1) |0\rangle
$$
(S-9)

Now, using

$$
\langle 0| \hat{d}_{k_1} \hat{d}_{k_2} \hat{d}_{k_3}^\dagger \hat{d}_{k_4}^\dagger |0\rangle = \delta_{k_1,k_4} \delta_{k_2,k_3} - \delta_{k_1,k_3} \delta_{k_2,k_4}
$$
(S-10)

leads to

$$
\rho_{el}(x_1, x_2, t) = \int dk_1 dp_1 dp_4 U_{\phi_{p_1} \varphi_{k_1}}^*(t) U_{\phi_{p_4} \varphi_{k_1}}(t) \phi_{p_1}^\dagger(x_1) \phi_{p_4}(x_1)
$$
$$
\int dk_2 dp_2 dp_3 U_{\phi_{p_2} \varphi_{k_2}}^*(t) U_{\phi_{p_3} \varphi_{k_2}}(t) \phi_{p_2}^\dagger(x_2) \phi_{p_3}(x_2)
$$
$$
- \int dk_1 dp_1 dp_3 U_{\phi_{p_1} \varphi_{k_1}}^*(t) U_{\phi_{p_3} \varphi_{k_1}}(t) \phi_{p_1}^\dagger(x_1) \phi_{p_3}(x_2)
$$
$$
\int dk_2 dp_2 dp_4 U_{\phi_{p_2} \varphi_{k_2}}^*(t) U_{\phi_{p_4} \varphi_{k_2}}(t) \phi_{p_2}^\dagger(x_2) \phi_{p_4}(x_1)
$$
(S-11)

We call these two terms $\rho_{el_1(x_1,x_2,t)}$ and $\rho^{int}(x_1, x_2, t)$ respectively; they can be rewritten as

$$
\rho_{el_1}(x_1, x_2, t) = \int dk \left| \int dp U_{\phi_p \varphi_k} \phi_p(x_1) \right|^2 \int dk \left| \int dp U_{\phi_p \varphi_k} \phi_p(x_2) \right|^2
$$
$$
= \rho_{el}(x_1, t) \rho_{el}(x_2, t)
$$
(S-12)
$$
\rho^{int}(x_1, x_2, t) = \left| \int dk_1 \int dp_1 U_{\phi_{p_1} \varphi_{k_1}}^* \phi_{p_1}^\dagger(x_1) \int dp_2 U_{\phi_{p_2} \varphi_{k_1}} \phi_{p_2}(x_2) \right|^2
$$

Similarly, we can derive Eq. (6) of the main text giving the number density for detecting two positrons

at the positions x_1 and x_2:

$$
\begin{aligned}
\rho_{po}(x_1, x_2, t) &= \int dp \left| \int dk U_{\varphi_k \phi_p} \varphi_k(x_1) \right|^2 \int \left| \int dk U_{\varphi_p \phi_k} \varphi_k(x_2) \right|^2 \\
&\quad - \int dp \left| \int dk_1 U^*_{\varphi_{k_1} \phi_p} \varphi^\dagger_{k_1}(x_1) \int dk_2 U_{\varphi_{k_2} \phi_p} \varphi_{k_2}(x_2) \right|^2 \\
&= \rho_{po_1}(x_1, x_2, t) - \rho^{int}_{po}(x_1, x_2, t) \\
&= \rho_{po}(x_1, t) \rho_{po}(x_2, t) - \rho^{int}_{po}(x_1, x_2, t)
\end{aligned}
\tag{S-13}
$$

The first term in Eq. (S-12) and Eq. (S-13) consists of the product of the number densities of one particle states calculated at the two positions x_1 and x_2 while the second term results from the exchange symmetry as can be seen from Eq. (S-10). This term is equal to the first term for $x_1 = x_2$ in absolute value and thus the number of couples is vanishing as can be seen in Figure 1.

1.2 Incoming particle

We now detail the derivations for the particle number density when an initial particle is present, given by Eq. (S-9) of the paper. The number density is defined by Eq. (6) of the paper, where the expectation value is taken over the state $|\zeta\rangle$ representing the initial particle wavepacket. Expanding this state in terms of modes created from the vacuum,

$$
|\zeta\rangle = \int dp \, \zeta_p(p_0, x_0) b^\dagger_p(0) |0\rangle ,
\tag{S-14}
$$

we are led as above to compute vacuum expectation values:

$$
\begin{aligned}
\rho_{el}(x, t) = \langle 0 | \int dp_2 dp_3 \int dp_1 \zeta^*_{p_1} b_{p_1} \phi^\dagger_{p_2}(x) \int dp'_2 \big(U^*_{\phi_{p_2} \phi_{p'_2}}(t) \hat{b}^\dagger_{p'_2} + U^*_{\phi_{p_2} \varphi_{p'_2}}(t) \hat{d}_{p'_2} \big) \\
\phi_{p_3}(x) \int dp'_3 \big(U_{\phi_{p_3} \phi_{p'_3}}(t) \hat{b}_{p'_3} + U_{\phi_{p_3} \varphi_{p'_3}}(t) \hat{d}^\dagger_{p'_3} \big) \int dp_4 \zeta_{p_4} b^\dagger_{p_4} |0\rangle
\end{aligned}
\tag{S-15}
$$

However, differently from the case where the initial state is vacuum, the terms containing the creation and annihilation operators $b^\dagger_p$ and b_p do not vanish when we have a wave packet. The surviving terms in this case give the number density:

$$
\begin{aligned}
\rho_{el}(x, t) &= \int dp_1 \ldots dp_4 \langle 0 | \zeta^*_{p_1} b_{p_1} \int dp'_2 U^*_{\phi_{p_2} \phi_{p'_2}}(t) \hat{b}^\dagger_{p'_2} \phi^\dagger_{p_2}(x) \phi_{p_3}(x) \int dp'_3 U_{\phi_{p_3} \phi_{p'_3}}(t) \hat{b}_{p'_3} \zeta_{p_4} b^\dagger_{p_4} |0\rangle \\
&\quad + \int dp_1 \ldots dp_4 \langle 0 | \zeta^*_{p_1} b_{p_1} \int dk'_2 U^*_{\phi_{p_2} \varphi_{k'_2}}(t) \hat{d}_{k'_2} \phi^\dagger_{p_2}(x) \phi_{p_3}(x) \int dk'_3 U_{\phi_{p_3} \varphi_{k'_3}}(t) \hat{d}^\dagger_{k'_3} \zeta_{p_4} b^\dagger_{p_4} |0\rangle \\
&= \int dp_1 \ldots dp_4 dp'_2 dp'_3 \langle 0 | \zeta^*_{p_1} U^*_{\phi_{p_2} \phi_{p'_2}}(t) \phi^\dagger_{p_2}(x) \phi_{p_3}(x) U_{\phi_{p_3} \phi_{p'_3}}(t) \zeta_{p_4} b_{p_1} \hat{b}^\dagger_{p'_2} \hat{b}_{p'_3} b^\dagger_{p_4} |0\rangle \\
&\quad + \int dp_1 \ldots dp_4 dk'_2 dk'_3 \langle 0 | \zeta^*_{p_1} U^*_{\phi_{p_2} \varphi_{k'_2}}(t) \phi^\dagger_{p_2}(x) \phi_{p_3}(x) U_{\phi_{p_3} \varphi_{k'_3}}(t) \zeta_{p_4} b_{p_1} \hat{d}_{k'_2} \hat{d}^\dagger_{k'_3} b^\dagger_{p_4} |0\rangle
\end{aligned}
\tag{S-16}
$$

Using the relations between the electron creation and annihilation operators, $\langle 0 | \hat{b}_{p_1} \hat{b}^\dagger_{p_2} |0\rangle = \delta_{p_1 p_2}$ (and similarly for the positronic ones) as well as the fact that the operators of different particles commute, one obtains the following number density:

$$
\begin{aligned}
\rho_{el}(x, t) &= \int dp_1 \ldots p_4 dp'_2 dp'_3 \zeta^*_{p_1} U^*_{\phi_{p_2} \phi_{p'_2}}(t) \phi^\dagger_{p_2}(x) \phi_{p_3}(x) U_{\phi_{p_3} \phi_{p'_3}}(t) \zeta_{p_4} \delta_{p_1 p'_2} \delta_{p'_3 p_4} \\
&\quad + \int dp_1 \ldots dp_4 dk'_2 dk'_3 \zeta^*_{p_1} U^*_{\phi_{p_2} \varphi_{k'_2}}(t) \phi^\dagger_{p_2}(x) \phi_{p_3}(x) U_{\phi_{p_3} \varphi_{k'_3}}(t) \zeta_{p_4} \delta_{p_1 p_4} \delta_{k'_2 k'_3} \\
&= \int dp_1 \ldots dp_4 \zeta^*_{p_1} U^*_{\phi_{p_2} \phi_{p_1}}(t) \phi^\dagger_{p_2}(x) \phi_{p_3}(x) U_{\phi_{p_3} \phi_{p_4}}(t) \zeta_{p_4} \\
&\quad + \int dk dp_1 dp_2 dp_3 \zeta^*_{p_1} U^*_{\phi_{p_2} \varphi_k}(t) \phi^\dagger_{p_2}(x) \phi_{p_3}(x) U_{\phi_{p_3} \varphi_k}(t) \zeta_{p_1}
\end{aligned}
\tag{S-17}
$$

yielding Eq. (S-9) of the paper:

$$= \int dk \left| \int dp U_{\phi_p \varphi_k}(t) \phi_p(x) \right|^2 + \left| \int dp_1 dp_2 \zeta_{p_1} U_{\phi_{p_2} \phi_{p_1}}(t) \phi_{p_2}(x) \right|^2. \tag{S-18}$$

We therefore see that despite the anti-symmetry of the Fock space state vectors, the electron number density can be parsed as a term equal to the density produced from vacuum excitation, given by Eq. (S-4), and a second term that represents the contribution of the wavepacket (this term vanishes when the ζ_p's are zero).

One can obtain the number of electrons by integrating the last equation with respect to x:

$$\begin{aligned} N_{el}(t) &= \int dp_1 \dots dp_4 \zeta_{p_1}^* U_{\phi_{p_2} \phi_{p_1}}^*(t) \delta_{p_2 p_3} U_{p_3 p_4}(t) \zeta_{p_4} \\ &+ \int dp_1 \dots p_4 dk \zeta_{p_1}^* U_{\phi_{p_2} \varphi_k}^*(t) \delta_{p_2 p_3} U_{\phi_{p_3} \varphi_k}(t) \zeta_{p_1} \\ &= \int dp_1 \dots dp_3 \zeta_{p_1}^* U_{\phi_{p_2} \phi_{p_1}}^*(t) U_{\phi_{p_2} \phi_{p_3}}(t) \zeta_{p_3} \\ &+ \int dp_1 \dots dp_3 dk \left| \zeta_{p_1} \right|^2 U_{\phi_{p_2} \varphi_k}^*(t) U_{\phi_{p_3} \varphi_k}(t) \end{aligned} \tag{S-19}$$

Notice that

$$\begin{aligned} \int dp_2 U_{\phi_{p_2} \phi_{p_1}}^*(t) U_{\phi_{p_2} \phi_{p_3}}(t) &= \int dp_2 \langle \phi_{p_1} | \hat{U}^\dagger(t) | \phi_{p_2} \rangle \langle \phi_{p_2} | \hat{U}(t) | \phi_{p_3} \rangle \\ &= \langle \phi_{p_1} | \hat{U}^\dagger(t) \mathbb{I} \hat{U}(t) | \phi_{p_3} \rangle - \int dk \langle \phi_{p_1} | \hat{U}^\dagger(t) | \varphi_k \rangle \langle \varphi_k | \hat{U}(t) | p_3 \rangle \\ &= \delta_{p_1 p_3} - \int dk U_{\varphi_k p_1}^*(t) U_{\varphi_k \phi_{p_3}}(t) \end{aligned} \tag{S-20}$$

where we used the fact that the identity can be expressed in terms of the basis as

$$\mathbb{I} = \int dp |\phi_p\rangle \langle \phi_p| + \int dk |\varphi_k\rangle \langle \varphi_k| \tag{S-21}$$

and since $\int dp \left| \zeta_p \right|^2 = 1$, one can rewrite the number of electrons as:

$$N_{el}(t) = 1 - \int dk \left| \int dp \zeta_p U_{\varphi_k \phi_p}(t) \right|^2 + \int dp dk \left| U_{\phi_p \varphi_k}(t) \right|^2 \tag{S-22}$$

The first term in Eq. (S-22) correspond to the electron wave packet (one electron). The second term corresponds to the Pauli blockade which takes place because of the incident wave packet such that the creation of the electron modes that exist in the wave packet is suppressed. The third term is the spontaneous creation resulting from exciting the vacuum by the electrostatic potential, the same as the number given in Eq. (S-5).

For the positron number density, one has similarly

$$\rho_{po}(x, t) = \int dp_1 dp_2 dk_1 dk_2 \langle 0 | \zeta_{p_1}^* \hat{b}_{p_1} \hat{d}_{k_1}^\dagger(t) \phi_{k_1}^\dagger(x) \phi_{k_2}(x) \hat{d}_{k_2}(t) \hat{b}_{p_2}^\dagger \zeta_{p_2} | 0 \rangle. \tag{S-23}$$

Now, using the expression of the time evolution of the positron creation operator Eq. (3) and keeping the surviving terms only, one obtains

$$\rho_{po}(x, t) = \int dk_1 dk_2 dp_1 dp_2 dp_1' dp_2' \langle 0 | \hat{b}_{p_1} \zeta_{p_1}^* U_{\varphi_{k_1} \phi_{p_1'}}(t) \hat{b}_{p_1'} \varphi_{k_1}(x) \varphi_{k_2}^\dagger(x) \rangle \hat{b}_{p_2'}^\dagger U_{\varphi_{k_2} \phi_{p_2'}}^*(t) \zeta_{p_2} \hat{b}_{p_2}^\dagger | 0 \rangle \tag{S-24}$$

Using

$$\begin{aligned} \langle 0 | \hat{b}_{p_1} \hat{b}_{p_1'} \hat{b}_{p_2'}^\dagger \hat{b}_{p_2}^\dagger | 0 \rangle &= \langle p_1, p_1' | p_2, p_2' \rangle \\ &= \delta_{p_1, p_2} \delta_{p_1', p_2'} - \delta_{p_1, p_2'} \delta_{p_1', p_2} \end{aligned}, \tag{S-25}$$

one obtains the positron number density given by Eq. (10) of the paper:

$$\rho_{po}(x,t) = \int dk \left| \int dp U_{\varphi_k \phi_p}(t) \phi_k(x) \right|^2 - \left| \int dk dp \zeta_p U_{\varphi_k \phi_p}(t) \phi_k(x) \right|^2 . \tag{S-26}$$

By integrating over all space the positron number

$$N_{po}(t) = \int dk dp \left| U_{\varphi_k \phi_p}(t) \right|^2 - \int dk \left| \int dp \zeta_p U_{\varphi_k \phi_p}(t) \right|^2 \tag{S-27}$$

The first term gives the number of positrons created spontaneously due to vacuum excitation as can be inferred by comparison with Eq. (S-7). The second term in Eq. (S-27) comes from the exchange symmetry, Eq. (S-25), involving the time-evolved amplitudes from the initial electron wavepacket modes.

2. NUMERICAL METHODS

We detail here how numerical results are computed from the expressions for the particle densities given above. The main quantities we need to obtain are the evolution operator amplitudes connecting initial and final field-free momentum states evolved in the presence of a barrier potential. These amplitudes $U_{\phi_p \varphi_k}$, defined in Eq. (4) of the main text, are obtained by splitting the Hamiltonian into parts acting in real space and in the momentum space alternatively (the split operator technique) [3, 4].

We start by defining our one-dimensional position space lattice of width Λ and of $N + 1$ sites,

$$X = \{0, \delta x, 2\delta x, ..., N\delta x\} \tag{S-28}$$

where $\delta x = \frac{\Lambda}{N}$ and the momentum lattice

$$P = \{-\frac{N}{2}\delta p, (-\frac{N}{2} + 1)\delta p, ... \frac{N}{2}p\}, \tag{S-29}$$

where $\delta p = \frac{2\pi}{\Lambda}$. We define the potential as a function of the position to obtain a vector $V(X)$. The basis vectors are calculated for each value $p = n\delta p$ were $n \in \{-\frac{N}{2}, -\frac{N}{2} + 1, ..., \frac{N}{2}\}$ and are given by:

$$\tilde{\phi}_p = N(p) \begin{pmatrix} 1 \\ \frac{cp}{mc^2 + E(p)} \end{pmatrix}$$
$$\tilde{\varphi}_p = N(p) \begin{pmatrix} -\frac{cp}{mc^2 + E(p)} \\ 1 \end{pmatrix} \tag{S-30}$$

where $N(p) = \frac{E(p) + mc^2}{2E(p)}$ normalizes the states $|p\rangle$ and $|n\rangle$ such that $\tilde{\phi}_p^\dagger \tilde{\phi}_p = \tilde{\varphi}_p^\dagger \tilde{\varphi}_p = 1$. We express each of the two elements of ϕ_p and φ_p in a way compatible with the usage of the Fast Fourier transform (FFT) algorithm i.e as a vector or list of values, all of them being zeros except for the nth one corresponding to $p = n\delta p$. Putting together all the basis states of positive energy, one obtains:

$$W_p = \mathrm{diag}\big(N(P)\big) \begin{pmatrix} \mathcal{I} \\ \mathrm{diag}\big(\frac{cP}{mc^2 + E(P)}\big) \end{pmatrix} \tag{S-31}$$

where $N(P)$ is the list of normalization constants $N(p)$ evaluated at all $p \in P$, $\mathrm{diag}\big(N(P)\big)$ is a diagonal matrix whose diagonal is $N(P)$, $\mathcal{I}$ is the unit matrix of dimensions $N \times N$ and $\mathrm{diag}\big(\frac{cP}{mc^2 + E(P)}\big)$ is a diagonal matrix whose nth diagonal element is $\frac{cp}{mc^2 + E(p)}$ with $p = n\delta p$. Similarly, we put together the basis vectors of negative energy.

$$W_n = \mathrm{diag}\big(N(P)\big) \begin{pmatrix} -\frac{cp}{mc^2 + E(p)} \\ \mathcal{I} \end{pmatrix} \tag{S-32}$$

Doing so, one can now use a time evolution operator represented by a matrix which is applied to all the states together. The time evolution operator which evolves the state from the instant t to $t + \delta t$ in

the split operator [3] scheme will be approximated to:

$$\hat{U}(\delta t) = e^{-i(H_k+V)\delta t} \approx e^{-iV\frac{\delta t}{2}} e^{-iH_k\delta t} e^{-iV\frac{\delta t}{2}}$$
$$= \hat{U}_V \hat{U}_k \hat{U}_V \tag{S-33}$$

where H_k is the kinetic part of the mechanical Hamiltonian and V is the potential energy. $U_k = e^{-i\hat{H}_k\delta t}$ acts in the Fourier space i.e. the momentum space and U_V acts in the position space. We use the fast Fourier transform and its inverse to make the transformation between the real and the Fourier spaces.

Since the Dirac free Hamiltonian i.e. the kinetic part of the full Hamiltonian is given by:

$$H_{D,k} = c\sigma_1 p + \sigma_3 mc^2 \tag{S-34}$$

where σ_1 and σ_3 are the Pauli matrices and using the definition of the exponential of a matrix, one finds:

$$U_k = 1 - i\hat{H}_{D,k}\delta t + \frac{1}{2!}\left(-i\hat{H}_{D,k}\delta t\right)^2 + \frac{1}{3!}\left(-i\hat{H}_{D,k}\delta t\right)^3 + ...$$
$$U_k = \sum_{n=0}^{\infty} \frac{1}{2n!}(-iH_{D,k}\delta t)^{2n} + \sum_{n=0}^{\infty} \frac{1}{(2n+1)!}(-iH_{D,k}\delta t)^{2n+1} \tag{S-35}$$

Now, using the properties of the Pauli matrices:

$$\sigma_1^2 = \sigma_3^2 = \mathbb{I}$$
$$\{\sigma_1, \sigma3\} = 0 \tag{S-36}$$

we find

$$\frac{1}{2n!}(-iH_{D,k}\delta t)^{2n} = (-1)^n \frac{1}{2n!}\delta t^{2n} E_p^{2n}\mathbb{I}$$
$$\frac{1}{(2n+1)!}(-iH_{D,k}\delta t)^{2n+1} = \frac{-i(-1)^n}{(2n+1)!}\delta t^{2n} E_p^{2n}\left(c\sigma_1 p + \sigma_3 mc^2\right)\delta t \tag{S-37}$$

Finally, using

$$\cos(\theta) = \sum_{n=0}^{\infty}(-1)^n \frac{\theta^{2n}}{2n!},$$
$$\sin(\theta) = \sum_{n=0}^{\infty}(-1)^n \frac{\theta^{2n+1}}{(2n+1)!}, \tag{S-38}$$

we can express the time evolution operator as a 2×2 matrix U whose elements are

$$U_{11} = \cos(E\delta t) - imc^2 \sin(E\delta t)/E$$
$$U_{12} = -icp\sin(E\delta t)/E$$
$$U_{21} = U_{12}$$
$$U_{22} = \cos(E\delta t) + imc^2 \sin(E\delta t)/E \tag{S-39}$$

Numerically, this matrix is interpreted as a $2N \times 2N$ matrix consisting of four blocks. Each of them is a diagonal matrix whose diagonal elements are calculated by evaluating U_{ij} for all the momentum values in P.

In order to implement this method, we wrote a MATLAB code computing the time evolution of QFT states on a lattice of size L that can take values in the order of a few atomic length units, discretized on a grid having $N_x = 2^{11}, 2^{12}$ or 2^{13} points (depending on the parameters of the problem). The code calculates at each instant of the discretized time, typically $n\delta t = n \times 10^{-6}$, the number densities defined above.

Note that the same method is used to calculate the time evolution of the bosonic QFT states where the kinetic klein-Gordon Hamiltonian is given by

$$H_{KG} = \left(\sigma_3 + i\sigma_2\right)\frac{\hat{p}^2}{2m} + \sigma_3 mc^2 3 \tag{S-40}$$

The kinetic time evolution operator becomes

$$U_{11} = \cos(E_p \delta t/\hbar) - \frac{i}{E_p}\sin(E_p \delta t/\hbar)\left(\frac{p^2}{2m} + mc^2\right)$$

$$U_{12} = \frac{-i}{E_p}\sin(E_p \delta t/\hbar)\frac{p^2}{2m}$$

$$U_{21} = -U_{12}$$

$$U_{22} = \cos(E_p \delta t/\hbar) + \frac{i}{E_p}\sin(E_p \delta t/\hbar)\left(\frac{p^2}{2m} + mc^2\right)$$

(S-41)

with the positive and negative energy solutions of the free Klein-Gordon equation being given by

$$\phi_p = N(p)\begin{pmatrix} mc^2 + E_p \\ mc^2 - E_p \end{pmatrix}$$

$$\varphi_p = N(p)\begin{pmatrix} mc^2 - E_p \\ mc^2 + E_p \end{pmatrix}$$

(S-42)

[1] S. S. Schweber, *An Introduction to Relativistic Quantum Field Theory*, (Dover, Mineola, 2005).
[2] F. Gelis and N. Tanji, Prog. Part. Nucl. Phys. 87, 1 (2016).
[3] F. Blumenthal and H. Bauke, J. Comp. Phys. 231, 454 (2012).
[4] J. W. Braun, Q. Su, and R. Grobe, Phys. Rev. A, 59, 604 (1999).